Materials and Structures, 1992, **25**, 212–218

Measurement of the fracture energy using three-point bend tests: Part 1—Influence of experimental procedures

G. V. GUINEA, J. PLANAS, M. ELICES

Departamento de Ciencia de Materiales, Escuela de Ingenieros de Caminos, Universidad Politécnica, Ciudad Universitaria, 28040 Madrid, Spain

Available measures of the fracture energy G_F obtained with the procedure proposed by RILEM TC-50 provide values that appear to change with sample size, calling into question the possibility of considering G_F as a material parameter. In this paper some possible sources of experimental errors, when the RILEM proposal is applied, are ascertained, namely the apparent energy dissipation from hysteresis in the testing equipment and energy dissipation in the lateral supports. It is concluded that either some other sources of energy dissipation are operative or that G_F cannot be considered a material property.

1. INTRODUCTION

For structural design, the relevance of the tensile fracture behaviour of quasi-brittle materials, such as concrete and cementitious materials, is well established and can be quantified by means of the fracture energy G_F (e.g. [1,2]). This is a useful parameter for design purposes, as pointed out in several examples by Hillerborg [3], as well as for modelling the fracture behaviour of cohesive materials, as reported in some recent reviews [4,5].

The most direct way of determining G_F is by means of a stable uniaxial tensile test. Unfortunately, it is difficult to perform stable and representative tensile tests [6] and a simpler procedure, based on the determination of the total work of fracture of three-point bend notched beams, was recently proposed by the RILEM Technical Committee TC-50 [7].

The performance of this test was analysed by Hillerborg [8]. After comparing the results for about 700 concrete beams of different sizes from 14 laboratories, he concluded that the proposed test method was suitable for use in testing laboratories with ordinary equipment, although a dependence of G_F on specimen size was detected. This size dependence was considered to be of no greater importance for the calculated strength of a structure than the corresponding size dependence in ordinary compressive strength tests.

However, a basic question still remains: will this size effect disappear by improving the experimental methods or, on the contrary, is this an intrinsic size effect and is G_F not a size-independent material property? The answer to this question will dictate the survival, in the concrete field, of the cohesive crack models and other fracture models that imply a constant, size-independent G_F.

The purpose of this paper, and of two subsequent ones, is to ascertain possible sources of experimental error when applying the RILEM procedures by analysing the contribution of the testing equipment, the sample characteristics and the experimental procedures to reach the final G_F value. Our analyses point towards the existence of an almost *size-independent* G_F value, which is obtained if the experimental procedures are refined according to the following results.

2. THE RILEM TEST

The purpose of this test is to measure the amount of energy absorbed when the specimen is broken into two halves. This energy is divided by the projected fracture area and the resulting value is assumed to be the fracture energy G_F. The ease of performing this test as well as the reliability of the test results will depend on the design of the test specimen and the details of the test procedure. The RILEM technical committee 50-FMC recommended the use of the three-point bend test on a notched beam. The procedure is explained elsewhere [7] and some relevant aspects will be briefly summarized here.

The size and dimensions of the recommended specimens (Fig. 1) were found by Hillerborg as a compromise between competing reasons. Since in our experiments some of the recommendations are apparently violated, it is interesting to remember the underlying reasons dictating the different specimen dimensions:

(a) The recommended *beam depths* of the specimens were chosen to keep the specimen as small as possible for a given aggregate size range. Notice that a single recommended beam depth exists for a given aggregate size. This was dictated by the convenience of keeping the volume of the specimen as small as possible relative to the area of the ligament, in order to minimize the influence of bulk energy dissipation.

(b) The large span-to-depth ratio of the recommendation was dictated by the interest in getting stable tests with testing machines working in position control. When closed-loop machines controlled in CMOD are available, the span-to-depth ratio becomes largely irrelevant. We used a span-to-depth ratio of 2.5 in the experiments presented in this work.

6. Van Gemert, D. A., 'Repairing of concrete structures by externally bonded steel plates', in Proceedings of ICP/RILEM/IBK International Symposium on Plastics in Material and Structural Engineering, Prague, 1982, pp. 519–526.
7. Klaiber, F. W., Dunker, K. F., Wipf, T. J. and Sanders, W. W., Jr, 'Methods of Strengthening Existing Highway Bridges', Transportation Research Board NCHRP Report (1987) 293.
8. Swamy, R. N., Jones, R. and Bloxham, J. W., 'Structural behaviour of reinforced concrete beams strengthened by epoxy-bonded steel plates', *Struct. Engnr* **65A**(2) (1987) 59–68.
9. Ranisch, E. H. and Rostasy, F. S., 'Bonded steel plates for the reduction of fatigue stresses of coupled tendons in multispan bridges', in 'Adhesion Between Polymers and Concrete', RILEM ISAP 86 (1986) pp. 561–570.
10. Meier, U., 'Bridge repair with high performance composite materials', *Mater. Technik* **4** (1987) 125–128.
11. Saadatmanesh, H. and Ehsani, M., 'Application of fiber-composites in civil engineering', in Proceedings of the sessions related to structural materials at Structures Congress '89, ASCE (1989) pp. 526–535.
12. Kaiser, H., 'Strengthening of Reinforced Concrete with Epoxy-Bonded Carbon-Fiber Plastics', doctoral thesis, ETH, Zurich (1989).
13. L'Hermite, R. and Bresson, J., 'Concrete reinforced with glued plates', in Proceedings of RILEM International Symposium on Synthetic Resins in Building Construction, Paris, 1967, pp. 175–203.
14. Lerchenthal, C. H., 'Bonded steel reinforcement for concrete slabs', *ibid.* pp. 165–173.
15. MacDonald, M. D., 'The Flexural Behaviour of Concrete Beams with Bonded External Reinforcement', TRRL Supplementary Report 415, Transport and Road Research Laboratory, Department of the Environment, Crowthorne, UK, 1978, p. 13.
16. Jones, R., Swamy, R. N., Bloxham, J. and Bouderbalah, A., 'Composite behaviour of concrete beams with epoxy bonded external reinforcement', *Int. J. Cement Compos. Lightwt Concr.* **2**(2) (1980) 91–107.
17. Jones, R., Swamy, R. N. and Ang, T. H., 'Under- and over-reinforced concrete beams with glued steel plates', *ibid.* **4**(1) (1982) 19–32.
18. Ladner, M., 'Reinforced concrete members with subsequently bonded steel sheets', in Proceedings of IABSE Symposium on Strengthening of Building Structures – Diagnosis and Therapy, Venezia, Final Report, Vol. 46 (1983) pp. 203–210.
19. Kent, D. C. and Park, R., 'Flexural members with confined concrete', *J. Struct. Div. ASCE* **97**(7) (1971) 1969–1990.
20. Knott, J. F., 'Fundamentals of Fracture Mechanics' (Butterworths, London, 1973).
21. Anandarajah, A. and Vardy, A. E., 'A theoretical investigation of the failure of open sandwich beams due to interfacial shear fracture', *Struct. Engr* **63B**(4) (1985) 85–92.
22. Triantafillou, T. C. and Gibson, L. J., 'Debonding in foam-core sandwich panels', *Mater. Struct.* **22** (1989) 64–69.
23. Hamoush, S. A. and Ahmad, S. H., 'Debonding of steel plate-strengthened concrete beams', *J. Struct. Engng ASCE* **116**(2) (1990) 356–371.
24. Ladner, M. and Weder, C., 'Concrete Structures with Bonded External Reinforcement', EMPA Report No. 705 (1981).

RESUME

Renforcement de poutres de béton armé par collage (colles époxy) de composites renforcés de fibres

Le renforcement externe de poutres de béton par collage de plastiques renforcés de fibres (FRP) semble un moyen adéquat d'accroître la capacité portante et la rigidité des constructions existantes. Les poutres de béton renforcées de FRP peuvent se rompre de différentes manières quand elles sont chargées en flexion. On identifie et on analyse dans cette étude les processus d'effondrement: fléchissement acier–rupture FRP, fléchissement acier–fragmentation du béton, rupture en compression et décollement.

Nous obtenons ici des équations décrivant chaque mécanisme de rupture en ayant recours à la méthode de déformation compatible, aux concepts de la mécanique de la rupture et à un modèle simple pour le mécanisme du décollement dû aux fissures de cisaillement. Ensuite, nous produisons des diagrammes montrant les calculs de poutre correspondant à chaque mécanisme de rupture, et nous examinons les effets des feuilles de FRP sur les caractéristiques de ductilité et de rigidité des composants renforcés.

En fin de compte, nous donnons les résultats d'essais de flexion quatre points sur des poutres en béton armé renforcées de diverses quantités de feuilles de carbone FRP unidirectionnelles (CFRP). Les résultats confirment l'analyse et soulignent le rôle important de la fissuration dans la délamination de la plaque composite par le processus de décollement. Il apparaît que ce processus impose une limite à l'épaisseur de la feuille composite au-delà de laquelle une rupture fragile se produit, sans que la capacité de flexion soit entièrement réalisée ni la ductilité assurée. On peut utiliser les résultats analytiques obtenus pour établir un processus de sélection de FRP pour le renforcement externe d'éléments de béton par des matériaux légers et durables.

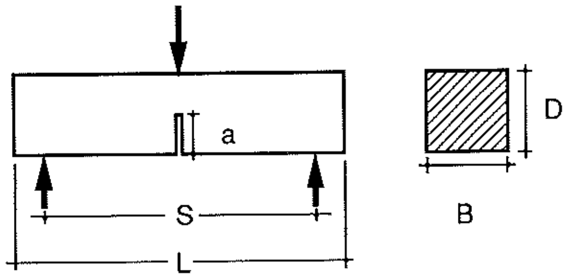

d_{max} (mm)	D (mm)	B (mm)	a (mm)	L (mm)	S (mm)
1.0 – 16.0	100 ± 5	100 ± 5	50 ±5	840 ±10	800 ± 5
16.1 – 32.0	200 ± 5	100 ± 5	100 ± 5	1190 ± 10	1130 ± 5
32.1 – 48.0	300 ± 5	150 ± 5	150 ± 5	1450 ± 10	1385 ± 5
48.1 – 64.0	400 ± 5	200 ±5	200 ± 5	1640 ± 10	1600 ± 5

Fig. 1 Notched beam geometry for fracture energy determination following the RILEM recommendation [7].

(c) The variable span-to-depth ratio of the recommendation was dictated by the need to keep the influence of the self-weight of the specimens within bounds, while keeping them as slender as possible. In our tests the self-weight is compensated, and hence this requirement need no longer hold.

(d) The notch-to-depth ratio was recommended to be 0.5 in order to keep the bulk energy dissipation small, while keeping the crack surface relatively large. In our specimens we wanted to analyse the influence of the bulk energy dissipation, and so we decreased the notch-to-depth ratio to 0.33.

In the recommendation, the displacement of the centre of the beam and the corresponding load are recorded until the beam falls down under its own weight. Then, the load–displacement curve is corrected for eventual non-linearities at low loads, and the energy supplied by the external load, W_0, represented by the area under the load–displacement curve, is measured as well as the displacement δ_0 at final fracture. The fracture energy is calculated from the expression

$$G_F = \frac{W_0 + mg\delta_0}{A_{lig}} \tag{1}$$

where g is the acceleration due to gravity, δ_0 the displacement at the final failure of the beam, A_{lig} the area of the initial ligament, $A_{lig} = (D - a)B$, and $m = m_1 + m_2$ where m_1 is the mass of the beam between supports and m_2 the mass of the part of the loading arrangement, not attached to the machine, that follows the beam during failure.

The term $mg\delta_0$ appearing in Equation 1 is required to take into account the work of the self-weight in the fracture process. In order to keep the experimental procedure as simple as possible, no weight compensation is suggested in the recommendation. However, weight compensation is feasible, and the correction in Equation 1 is only an approximation derived by Petersson [9], who experimentally checked it by comparison with weight-compensated tests.

In weight-compensated tests such as those performed by the authors, the full load–displacement curve is obtained (in principle) and the fracture energy is

$$G_F = \frac{W}{A_{lig}} \tag{2}$$

where W is the total work of fracture, given by the area under the complete load–displacement curve [9].

Actual experimental arrangements may differ appreciably from the ideal design, and moreover there is always a limit to the accuracy of the measurements. In the following we review possible sources of error due to the testing equipment, the sample properties and the measurement procedures.

3. HYSTERETIC BEHAVIOUR OF THE EXPERIMENTAL EQUIPMENT

In a loading–unloading process, the experimental equipment may display hysteresis. The area of the hysteresis loop (in the load–displacement representation) is equivalent to an extra energy added to the true fracturing energy. Hysteresis may proceed from different sources:

(a) true mechanical energy dissipation (due to the inclusion of inelastic joints in the displacement measurement, for example);

(b) transducer hysteresis (coupled with electronic hysteresis of the amplifiers and signal conditioners); and

(c) recorder hysteresis (either electronic or mechanical).

If not taken properly into account, hysteresis will deliver fracture energies larger than the actual ones. Since hysteresis usually depends on the maximum load, it may introduce a spurious size effect in the measurement of G_F.

An easy way to evaluate the significance of this hysteresis is to perform standard tests with materials of a well-known linear elastic response in the expected range of loads. This calibration test should mimic the standard test, except in the material to be tested. In particular, load and displacement measurements should be performed as in the standard test.

Our experimental system was calibrated using this procedure by testing steel and aluminium beams [10,11]. A small hysteresis cycle, depending on the maximum load, was observed, and the results are shown in Fig. 2a. It is worth noting that the dissipated energy due to equipment hysteresis corresponding to the maximum load recorded on testing concrete beams was less than 10 mJ. As we will show in a subsequent paper [12], when analysing experimental results for concrete, this figure contributes less than 0.6% to the G_F value. The relative error introduced in the specific energy determination is shown in Fig. 2b. The reference value is $G_F = 81\ \mathrm{N\,m^{-1}}$, the corrected experimental specific fracture energy obtained in our tests [12]. Although very small in our case, this contribution cannot be neglected *a priori* and calibration tests are recommended.

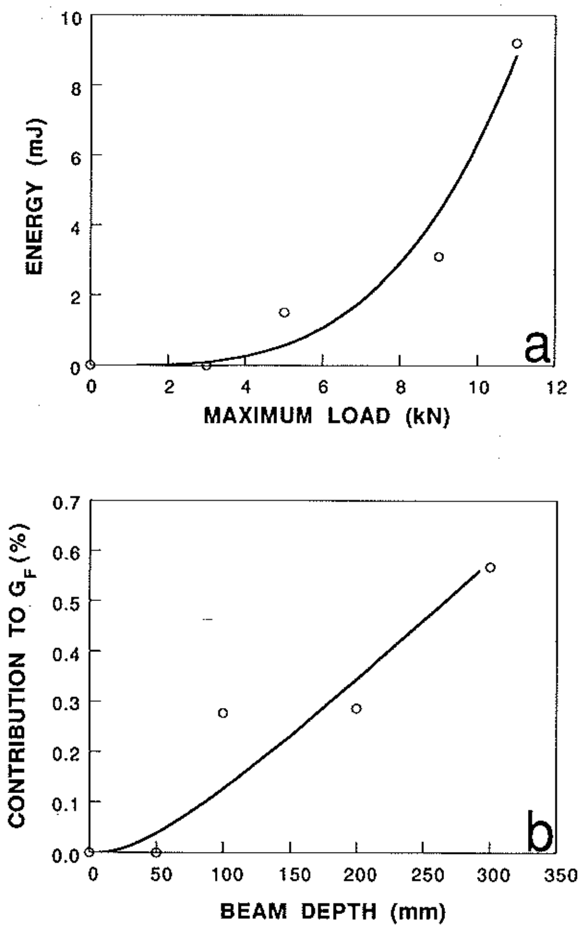

Fig. 2 Measured contribution of the hysteresis of the experimental equipment to the overall energy measurement: (a) absolute value, (b) relative contribution to the fracture energy. Reference value, $G_F = 81\ \mathrm{N\,m^{-1}}$.

4. INFLUENCE OF THE SAMPLE PREPARATION PROCEDURE

Actual samples have suffered a number of disturbances during their preparation, which may have a different influence on small and on larger samples, hence introducing a size effect on the fracture energy. Apart from this size effect, two different specimen preparation procedures may deliver different values of G_F for a given specimen size. Two cases are considered here; the presence of a notch instead of an ideal crack, and the heterogeneity introduced when casting the samples in moulds.

Notched beams and precracked beams were compared by Swartz and co-workers [13,14]. Eighty-four beam specimens were tested, one-half precracked and one-half notched, and it was found that failure loads were higher for cracked beams than for notched beams, but differences in G_F, obtained using Equation 1, were not significant when compared with the differences in G_F for several values of the notch-to-depth ratio.

Concrete samples are made by casting in moulds or by sawing from a previously moulded bigger plate. Both procedures may induce heterogeneities in the samples; casting favours segregation at the edges (skin effect) and sawing produces damage. Obviously, the importance of these heterogeneities decreases with increasing specimen size. To ascertain the influence of both procedures on G_F, two sets of eight samples – one set moulded and another cut from a plate – were tested following the RILEM recommendations. No significant differences were found in the results [11].

5. EXPERIMENTAL PROCEDURES

Actual experimental arrangements differ from the ideal design, and also material behaviour may show some departure from the idealized model. Attention will be paid to three possible sources of experimental error that may influence the measurement of G_F: non-ideal boundary conditions at the supports, non-ideal behaviour of bulk material – more specifically, the influence of bulk energy dissipation –, and non-ideal performance of the RILEM test. The last two problems will be dealt with in two subsequent papers and the first one is considered here.

5.1 Energy dissipation at beam rolling supports

Lateral supports are sensitive devices, as is well known when testing beams. Energy can be dissipated due to beam damage around the supports and due to friction during the test. Indeed, the RILEM draft recommendation [7] is quite specific about the necessity of avoiding inclusion of energy dissipated at the supports. To do so requires the displacement of the central section of the beam to be measured not relative to the supports, but relative to points of the beam above the supports (away from them). In this way the inelastic displacements due to crushing are excluded from the measurement. The recommendation accepts measurement relative to the support only if it has been proved that the corresponding inelastic displacements are less than 0.01 mm. It is also clear from the recommendation that the supports must be rolling supports, not fixed. Despite their clarity, these recommendations are not always fulfilled in the experiments reported in the literature. One of the aims of the present work is to show quantitatively that they have to be taken into account.

In a rolling support a mixture of indentation and friction during rolling makes the analysis very involved. In addition, the difficulty of a numerical analysis increases when it is considered that the details of the rollers and the material behaviour of the beam play an important role. Such problems prompted us to look for an experimental approach to measure the dissipated energy.

However, previous to the experimental work, an upper bound for the dissipated energy due to friction was estimated under the hypothesis of fixed supports. Although such a testing procedure is not recommended, fixed supports are frequently quoted in test reports. To evaluate the dissipated energy, a numerical simulation of the test was made. With the help of the computer code ANSYS® the beam was modelled as a cohesive material

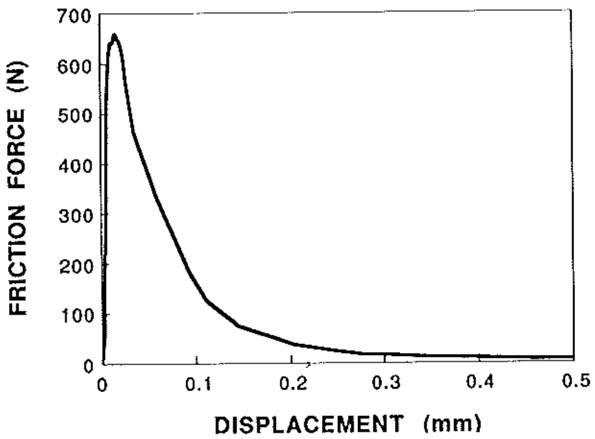

Fig. 3 Computed evolution of the frictional force at a fixed support versus the relative displacement of the contacting points. Beam depth = 50 mm, loading span = 125 mm, beam thickness = 100 mm, notch depth = 17 mm, $f_t = 3.14$ MPa, $E = 27$ GPa, $G_F = 100$ N m^{-1}, bilinear softening curve according to Petersson [9].

[4]. A bilinear softening function shaped like that of Petersson [9] was used to describe the fracture zone, and the bulk was considered linear elastic. Concrete properties were $E = 27$ GPa, $\nu = 0.2$, $G_F = 100$ N m^{-1}, $f_t = 3.14$ MPa and critical opening $w_c = 114.6$ µm. Friction was modelled according to Coulomb behaviour, allowing sliding when the tangential load equals the product of the normal load by the friction coefficient μ. A value of $\mu = 0.3$ was chosen. This is a typical value for steel-on-steel friction, and a lower bound for steel-on-rock friction. This is also an approximate value for the specific supports used by the authors, as determined by Guinea [11]. Friction loads versus corresponding displacement were computed for the four sizes of tested beams (as reported in the third paper of this series [12]), where $D/S = 0.4$, $a/D = 0.33$ and $B = 100$ mm. A typical plot for beams with $D = 50$ mm is shown in Fig. 3. Twice the area under this curve gives the dissipated energy due to friction during the test. This value amounts to 30% of the fracture energy G_F, for the four sizes considered.

These results agree with a rough estimate, previously made by two of the authors [15], by assuming simplified rigid-body kinematics, as shown in Fig. 4. A straightforward analysis shows that the total external work, W^E, supplied to the beam is

$$W^E = W - 2\mu \frac{D}{S} W \tag{3}$$

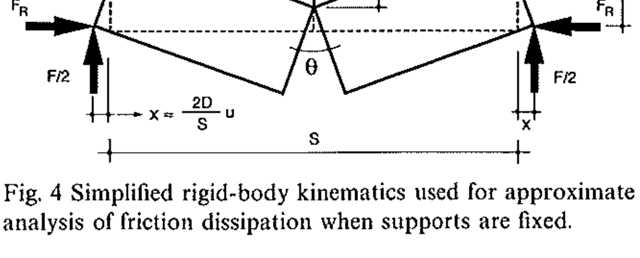

Fig. 4 Simplified rigid-body kinematics used for approximate analysis of friction dissipation when supports are fixed.

where W is the work done by the central load alone and D/S is the depth-to-span ratio.

The blind use of Equation 2 leads to a 'measurement' of the fracture energy G_{FMeas} which differs from the true value of the fracture energy, G_F, which should take into account the external energy only; hence

$$G_{FMeas} = G_F \frac{1}{1 - 2\mu(D/S)} \tag{4}$$

so that the relative error in G_F amounts to

$$\frac{\Delta G_F}{G_F} = \frac{G_{FMeas} - G_F}{G_F} = \frac{2\mu(D/S)}{1 - 2\mu(D/S)} \tag{5}$$

If $D/S = 0.4$ – as in our tests – and $\mu = 0.3$, the relative error is 32%, in agreement with the more involved estimation based on finite-element computations. The relative error is lower – between 8 and 15% – when samples with the recommended RILEM geometries are used. These results warn us against neglecting friction during testing because relative errors may be large, even when rolling is allowed, as is shown below.

To evaluate energy dissipation during rolling of the supports, a testing device that allows measurement of normal and tangential forces and their associated displacements was designed and built. This device is shown in Figs 5 and 6. The normal force is applied, by means of a 1275 Instron servohydraulic machine, through rollers with an overall friction coefficient of 0.003. To avoid bending of the upper loading rod, the lateral load has to be applied as close as possible to the lower specimen bottom. In this way the support reaction and the lateral load give a combined vertical loading with zero off-axis eccentricity.

The test was run in such a way that the variations with time of the normal load and of the tangential displacement were coincident with those previously recorded in a beam test for the lateral support (the normal load on the support was taken to be half the central load and the displacement at the support was taken to be half the crack mouth opening displacement, CMOD). The rolling support was the same as for the beam tests and the concrete sample was from the same concrete batch. Details of the experimental set-up are given elsewhere [11].

Test results are shown in Fig. 7. These are typical results from one of the 11 tests carried out. Fig. 7a shows the evolution of the tangential load with the corresponding tangential displacement (input), and Fig. 7b the evolution of the normal load (input) with the normal displacement. From these results the total dissipated work at the rolling support, due to normal and shear forces, can be evaluated. Work due to normal forces is mainly due to crushing of concrete, and work due to tangential forces is mainly due to friction. The energy dissipated at the supports is shown in Fig. 8a as a function of the maximum load. This figure was drawn from 11 test results using inputs from beam tests of four different sizes. The relative influence of the dissipation at the supports on the measured value of G_F

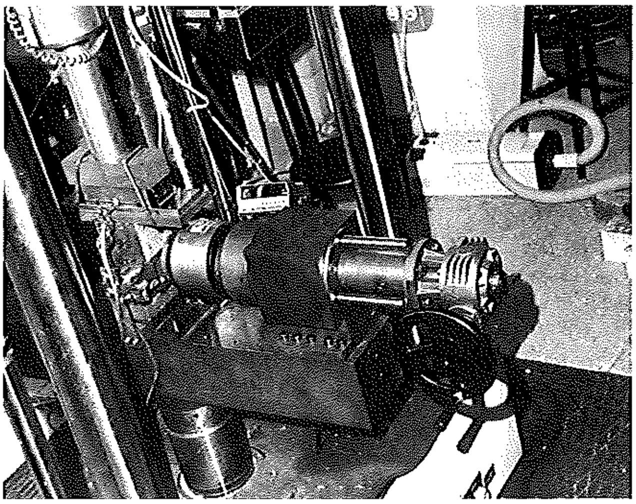

Fig. 5 Photograph of the biaxial loading device used in the experimental investigation of the rolling support.

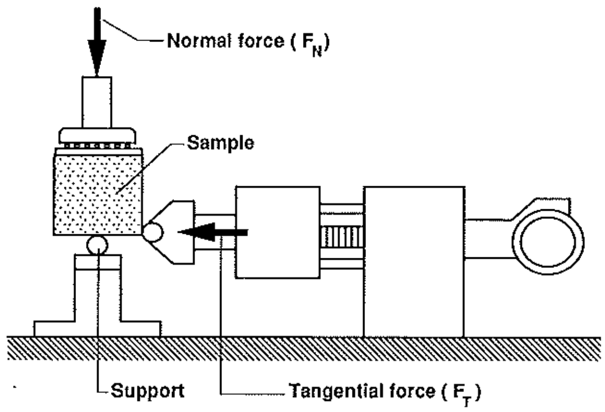

Fig. 6 Scheme of the biaxial loading device used in the experimental investigation of the rolling support.

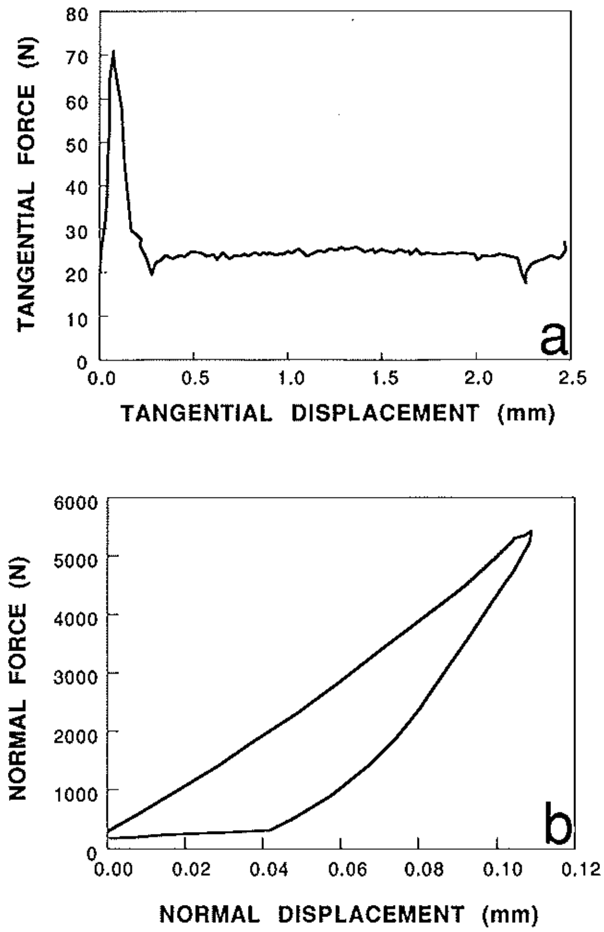

Fig. 7 Output of a test on the rolling support: (a) tangential force versus tangential displacement curve, (b) normal force versus normal displacement curve.

is size-dependent, as is shown in Fig. 8b. For our experiments, its relative influence is less than 20%.

The above results show that crushing at the supports may be an important source of energy dissipation and that the strict requirements set in section 4.3 of the RILEM draft recommendation [7] are indeed essential. However, it appears that they are not enough, because in the RILEM draft the rolling friction is not taken into account. The rolling friction is not high for the major part of the test, as shown in Fig. 9 (drawn from Figs 7a and b) which indicates that the ratio F_T/F_N is of the order of 0.01, as expected for rolling. However, this relationship is not constant and becomes very large for small normal loads. When the energy dissipated by the tangential force is computed from Fig. 7a, the result shown in Fig. 10a is obtained. Fig. 10b shows the relative contribution to the measured fracture energy, a contribution that turns out to be non-negligible.

6. CONCLUSIONS

So far, several sources of energy dissipation have been found. All of them, if not taken properly into account, may influence the measured value of the specific fracture energy G_F.

1. There is an apparent energy dissipation coming from hysteresis in the testing equipment. Its influence is specimen size-dependent. For a series of concrete tests and equipment this energy contributes less than 0.6% to the G_F value. However, this contribution cannot be neglected *a priori* and calibration tests are recommended.
2. Sample preparation should influence G_F values. Nevertheless, no clear difference was observed between results for notched beams and those for precracked beams. The same conclusion applies to the results for moulded beams and those for beams sawn from a larger plate.
3. If the lateral supports are fixed, frictional dissipation may introduce very large errors in the measurement of the fracture energy. Only tests with rolling supports should be accepted in G_F measurements.

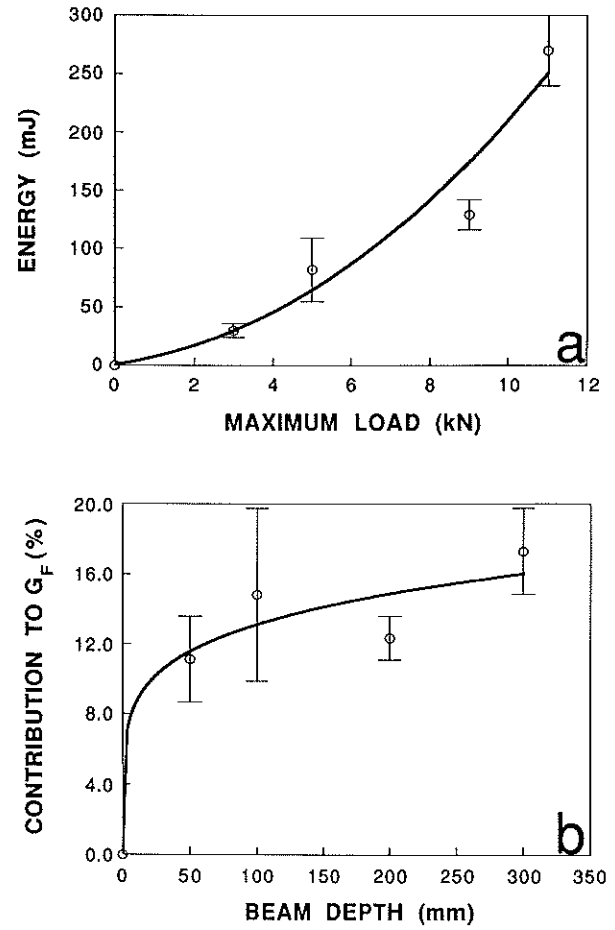

Fig. 8 Total energy dissipated at the rolling supports: (a) absolute value, (b) relative contribution to the measured fracture energy. Reference value, $G_F = 81\ \mathrm{N\,m^{-1}}$.

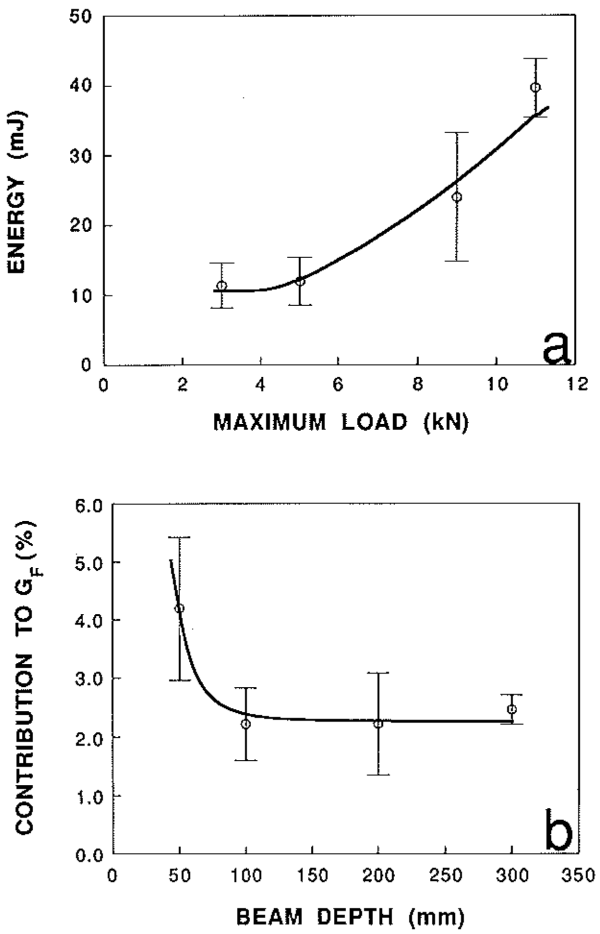

Fig. 10 Energy dissipated at the rolling supports by the tangential force: (a) absolute value, (b) relative contribution to the measured fracture energy. Reference value, $G_F = 81\ \mathrm{N\,m^{-1}}$.

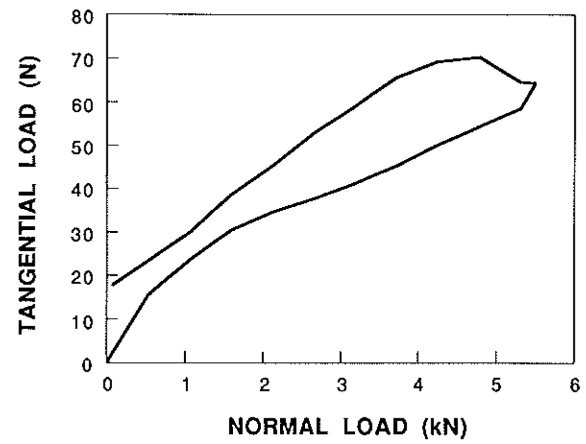

Fig. 9 Experimental relationship between the normal and the tangential load in the rolling support.

4. Even with rolling supports there is some energy dissipation at the supports, partly due to concrete crushing, and partly due to friction. Direct measurement of such energy indicates that its influence on the measured G_F is not negligible, and that this influence is dependent on the specimen size. Even when the crushing component is excluded from the measurement, a non-negligible energy dissipation is produced by rolling friction.

5. Because the measured G_F increases by more than 50% when the size is increased three times [12], we must conclude that the above corrections are not enough to imply a constant value for G_F. This means either that some other sources of energy dissipation are operative, or that G_F cannot be considered a material property.

In the forthcoming paper, bulk energy dissipation is analysed as a possible source of the apparent size dependence of G_F.

ACKNOWLEDGEMENTS

The authors gratefully acknowledge financial support for this research provided by the Comisión Interministerial de Ciencia y Tecnología CICYT, Spain, under grant PB86-0494, and by the Universidad Politécnica de Madrid under grant A-91 0020 02-31.

REFERENCES

1. Wittmann, F. H. (ed.), 'Fracture Toughness and Fracture Energy of Concrete' (Elsevier, Amsterdam, 1986).
2. Mihashi, H., Takahashi, H. and Wittmann, F. H. (eds), 'Fracture Toughness and Fracture Energy: Test Methods for Concrete and Rock' (Balkema, Rotterdam, 1989).
3. Hillerborg, A., 'The theoretical basis of a method to determine the fracture energy G_F of concrete', *Mater. Struct.* **18**(106) (1985) 291–296.
4. Elices, M. and Planas, J., 'Material models', in 'Fracture Mechanics of Concrete Structures' (Chapman and Hall, London, 1989) pp. 16–66.
5. *Idem*, 'Size effect and experimental validation of available fracture models', in 'Analysis of Concrete Structures by Fracture Mechanics' (Chapman and Hall, London, 1990) pp. 99–127.
6. Hordijk, D. A., 'Deformation-Controlled Uniaxial Tensile Tests on Concrete', Delft University of Technology Report 25.5.89-15 VFA (1989).
7. RILEM TC-50 FMC (Draft Recommendation), 'Determination of the fracture energy of mortar and concrete by means of three-point bend tests on notched beams', *Mater. Struct.* **18**(106) (1985) 285–290.
8. Hillerborg, A., 'Results of three comparative test series for determining the fracture energy G_F of concrete', *ibid.* **18**(107) (1985) 407–413.
9. Petersson, P. E., 'Crack Growth and Development of Fracture Zones in Plain Concrete and Similar Materials', Report TVBM-1006 (Division of Building Materials, University of Lund, Sweden, 1981).
10. Planas, J. and Elices, M., 'Towards a measure of G_F: an analysis of experimental results', in 'Fracture Toughness and Fracture Energy of Concrete', edited by F. H. Wittmann (Elsevier, Amsterdam, 1986) pp. 381–390.
11. Guinea, G. V., 'Medida de la Energía de Fractura del Hormigón', PhD thesis, E.T.S. Ingenieros de Caminos, Universidad Politécnica de Madrid (1990).
12. Elices, M., Guinea, G. V. and Planas, J., 'Measurement of the fracture energy using three-point bend tests: 3 – Influence of cutting the P–δ tail', *Mater. Struct.* (1992) in press.
13. Swartz, S. E., Hu, K. K., Fartash, M. and Huang, C. M. J., 'Stress intensity factor for plain concrete in bending prenotched versus precracked beams', *Exper. Mech.* **22**(11) (1982).
14. Swartz, S. E. and Refai, T. M. E., 'Influence of size effects in opening mode fracture parameters for precracked concrete beams in bending', in 'Fracture of Concrete and Rock' (Springer, 1989) pp. 242–254.
15. Planas, J. and Elices, M., 'Conceptual and experimental problems in the determination of the fracture energy of concrete', in 'Fracture Toughness and Fracture Energy: Test Methods for Concrete and Rock', edited by H. Mihashi, H. Takahashi and F. H. Wittmann (Balkema, Rotterdam, 1989) pp. 165–181.

RESUME

Mesure de l'énergie de rupture par des essais en flexion trois points: 1 – Influence des méthodes expérimentales

L'expérience montre que l'énergie de rupture spécifique G_F est un paramètre de calcul pour le béton et les matériaux à base de ciment. Cependant, il apparaît que les valeurs des mesures de l'énergie de rupture G_F obtenues selon la méthode préconisée par la Commission Technique 50 de la RILEM, dont on dispose, changent avec la taille de l'éprouvette, ce qui met en question la possibilité de considérer G_F comme un paramètre du matériau. Dans cet article, on a mis au jour plusieurs sources de dissipation de l'énergie qui, toutes, si on n'en tient pas compte comme il convient, risquent d'influer sur la valeur de l'énergie spécifique G_F.

Il existe une dissipation de l'énergie apparente dans le dispositif d'essai due à l'hystérésis dont l'influence dépend de la taille de l'éprouvette. Bien que dans le dispositif expérimental des auteurs l'hystérésis soit très bas, on ne peut a priori *négliger cet élément et on recommande des essais d'étalonnage. Si les supports latéraux sont fixés, la dissipation due au frottement peut introduire des erreurs importantes dans la mesure de l'énergie de rupture. Pour mesurer G_F, il faudrait accepter seulement des essais avec des supports roulants et, même dans ce cas, il y a une dissipation de l'énergie non négligeable en rapport avec la taille de l'éprouvette.*

Bien que les effets considérés ci-dessus introduisent des erreurs de G_F, et contribuent à son effet d'échelle, on conclut que soit d'autres sources de dissipation de l'énergie interviennent, soit G_F ne peut être considéré comme une propriété du matériau.